International Journal of Rock Mechanics & Mining Sciences 60 (2013) 82–94

Contents lists available at SciVerse ScienceDirect

International Journal of Rock Mechanics & Mining Sciences

journal homepage: www.elsevier.com/locate/ijrmms

A rock engineering systems based model to predict rock fragmentation by blasting

F. Faramarzi, H. Mansouri *, M.A. Ebrahimi Farsangi

Mining Engineering Department, Shahid Bahonar University of Kerman, Kerman, Iran

ARTICLE INFO

Article history:
Received 12 March 2012
Received in revised form
12 December 2012
Accepted 29 December 2012
Available online 30 January 2013

Keywords:
Blasting
Rock fragmentation
Rock engineering systems
Kuz–Ram model
Regression modeling
Sungun copper mine

ABSTRACT

A new model for prediction of rock fragmentation by blasting is presented based upon the basic concepts of rock engineering systems (RES). The newly proposed approach involves 16 effective parameters on fragmentation by blasting with keeping simplicity as well. The data for 30 blasts, carried out at Sungun copper mine, western Iran, were used to predict fragmentation by the RES based model as well as Kuz–Ram and multiple regression modeling. To validate the new model, the fragmentations of nine production blasts were measured and the results obtained were compared with the predictions carried out by the RES, Kuz–Ram and multiple regression models. Coefficient of determination (R^2) and root mean square error (RMSE) were calculated for the models to compare the results obtained. For the RES, linear, polynomial, power, logarithmic, exponential and Kuz–Ram models, R^2 and RSME are equal to (0.65 and 14.51), (0.58 and 29.73), (0.54 and 21.58), (0.60 and 32.64), (0.61 and 23.80), (0.50 and 184.60) and (0.46 and 22.22) respectively. These indicate that the RES based model predictor with higher R^2 and less RMSE performs better than the other models.

1. Introduction

Rock fragmentation has been the concern of many research works because it is considered as the most important aspect of production blasting, since it affects on the costs of drilling, blasting and the efficiency of all the subsystems such as loading, hauling and crushing in mining operations [1–7]. The parameters affecting on the rock fragmentation can be categorized in two groups: the first group is controllable parameters; such as blasting design parameters and also explosive related parameters; and the second one are uncontrollable parameters, which contains physical and geomechanical properties of intact rock and also rock mass [8–10].

Prediction of the rock fragmentation size is the first step toward optimization of blast design parameters to produce required fragment size [11]. Several studies have been conducted on the prediction of fragmentation by blasting accounting for controllable and uncontrollable parameters. An equation on the basis of the relationship between mean fragment size and specific charge was developed by Kuznetsov [12]. Cunningham [13], based upon the Kuznetsov model and the Rosin & Rammler distribution, introduced a new model, Kuz–Ram model, to predict rock fragmentation by blasting. Kuz–Ram model was further improved by Cunningham [14].

Hjelmberg [15] presented the SveDeFo model to predict X_{50}, considering the rock mass type and the blast pattern. Otterness et al. [16] performed an extensive study to correlate shot design parameters to fragmentation. Kou and Rustan [17] developed an empirical model to predict X_{50}. Lownds [18] used distribution of explosives energy to predict the fragmentation by blasting. Aler et al. [4] carried out a research work to predict blast fragmentation by multivariate analysis procedures. Djordjevic [19] presented the results of blast fragmentation modeling based on two mechanism of failure at JKMRC. Furthermore, Morin and Ficarazzo [20] applied Monte Carlo simulation as a tool for prediction of fragmentation based on Kuz–Ram model. Also, Gheibie et al. [21,22] tried to enhance fragmentation prediction by modification of Kuznetsov model and Kuz–Ram model. In 2010, Ouchterlony proposed a new fragment size distribution function [23].

Some research works were carried out using artificial intelligence methods to predict rock fragmentation. Saavedra et al. [24] conducted a research work to predict fragmentation by blasting, using a neural network model. Monjezi et al. [25] developed a fuzzy logic model for prediction of rock fragmentation by blasting. Kulatilake et al. [10] presented a piece of work, predicting mean particle size in rock blast fragmentation using neural networks. Also, Monjezi et al. [26] used neural networks for prediction of rock blasting fragmentation. Chakraborty et al. and Hudaverdi et al. [27,28] applied multivariate analysis procedures to predict rock fragmentation by blasting.

The empirical and neural network models that are based upon the data surveying from different blasting operations, in a certain

* Corresponding author. Tel.: +98 341 211 2764; fax: +98 341 212 1003.
E-mail addresses: hmansouri@uk.ac.ir, hmansuri2000@yahoo.fr (H. Mansouri).

1365-1609/$ - see front matter © 2013 Elsevier Ltd. All rights reserved.
http://dx.doi.org/10.1016/j.ijrmms.2012.12.045

range of rock types, cannot be generalized for various ground conditions. Furthermore, all of above models do not simultaneously consider all the pertinent parameters in the modeling. Under such limitations or constraints, the prediction of rock fragmentation due to blasting needs the new innovative methods such as the RES based model, capable of accounting unlimited parameters in the model. The RES approach has been applied to a number of rock engineering fields, for examples, evaluation of stability of underground excavations [29], hazard and risk assessment of rockfall [30], rock mass characterization for indicating natural slope instability [31], development of an assessment system for blastability of rock masses [32], assessing geotechnical hazards for TBM tunneling [33] and quantitative hazard assessment for tunnel collapses [34].

Fig. 1. A general view of the Sungun copper mine.

The present paper introduces a new RES based model that can be applied to evaluate fragmentation risk (poor fragmentation) and then, predict rock fragmentation in bench blasting, considering all pertinent parameters. To validate the performance of the model proposed, it is applied to Sungun copper mine, Iran. Furthermore, the results obtained are compared with the results of Kuz–Ram model and also statistical modeling, which carry out for the same mine.

2. The field study

2.1. Site description

Sungun copper mine, an open-pit mine, with a mineable reserve of 410 Mt and average grade of 0.6% copper, is located 100 km north east of Tabriz city, Iran. It is planned to produce 7 Mt ore for the initial 7 years with the intention to expand capacity up to 14 Mt of ore. A maximum slope height of 765 m was obtained for the initial design of the final pit. In blasting operation, ANFO is used as explosive and NONEL and detonating cord as initiation systems with staggered pattern. Also, inter-row

Table 1
Properties of intact rock and rock mass in the Sungun copper mine [35].

Sector	Average values of intact rock and rock mass			
	UCS (MPa)	*C* (KPa)	GSI	RMR
RS01	55	538	35	37
RS02	63	630	38	49
RS03	73	662	39	44
RS04	68	710	39	34
RS05	64	655	37	43
RS06	87	794	39	41
RS07	82	789	40	44

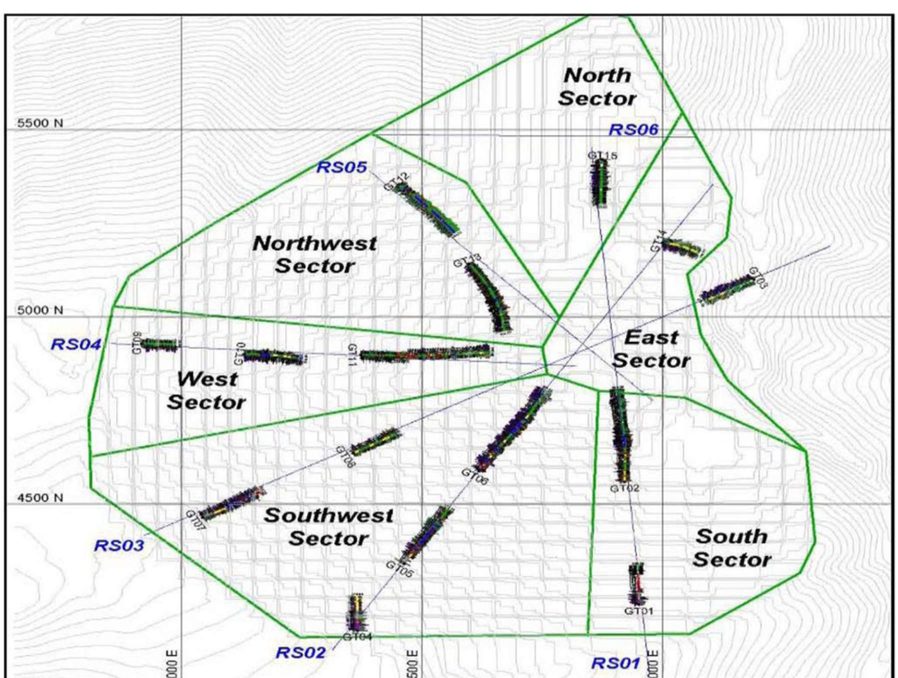

Fig. 2. Different sectors in the Sungun copper mine [35].

sequencing was adopted. A general view of Sungun copper mine is shown in Fig. 1.

The geology of area consists of Sungun intrusive complex hosting the Sungun porphyry copper stock intruded along the Sungun anticline into cretaceous limestone, marls and shales. The main lithological units exposed in the Sungun pit are Sungun porphyry (SP), Dykes, Pyroclastics (PC), Trachybasalt (TB) and Skarn (SK) [35].

2.2. Rock mass properties

Based upon the rock mass characteristics in the Sungun copper mine, seven sectors were recognized (RS01–RS07), as shown in Fig. 2 and Table 1 [35].

2.3. Data collection

Based upon 39 blasts carried out at Sungun copper mine, a database was prepared for models development. Out of 39 blasts, 30 blasts were used for modeling development and nine blasts for evaluation of models performance. In this database, burden (B), maximum instantaneous charge, powder factor, S/B (S: spacing), S_T/B (S_T: Stemming), stiffness factor, time delay, number of rows, blasthole inclination, blasthole deviation, blasthole diameter (D), B/D, J/B (J: subdrilling), blasting pattern, initiation sequence and blastability index were measured or calculated as input parameters to the model and X_{80} (80% passing size) as representative of muck pile fragmentation size was measured as a favorable parameter in each blasting round.

The image analysis technique was used to find muck pile distribution and the relevant X_{80} for each blast. In average, for each blast 30 photos were taken systematically from muck pile in different steps of loading (immediately after blast, after loading half of muck pile and at the end of muck pile loading). Goldsize software was used to carry out image analysis in which delineating of fragments is done manually and the fine correction option was used. The software was calibrated by comparing image analysis with sieve results (for determining sieve shift and mass power). A sample work of the image analysis for a blast (blast no. 9) at Sungun copper mine and the corresponding muck pile distribution curve are shown in Figs. 3 and 4 respectively.

The basic descriptive statistics of 39 blasts carried out at Sungun copper mine are summarized in Table 2.

3. Muck pile fragment size prediction, using Kuz–Ram model

The Kuz–Ram model, proposed by Cunningham [14], is the most used empirical fragmentation method, based upon the Kuznetsov and Rosin–Rammler equations. The Rosin–Rammler equation is used to characterize muck pile size distribution. It is expressed as an exponential relation [13]:

$$R = e^{-(x/x_c)^n} \tag{1}$$

where R is the weight fraction of fragments larger than x, n is the uniformity exponent, x_c is the characteristic size and x is the fragment size.

The Kuznetsov [12] equation is a semi-empirical equation based upon field studies and that relates the mean fragment size to the quantity of explosive, the rock volume blasted and the rock strength:

$$X_m = A\left(\frac{V_O}{Q_T}\right)^{0.8} Q_T^{0.167} \tag{2}$$

where X_m is the mean fragment size (cm), A is the rock factor, V_O is the rock volume fragmented per blasthole (m^3), Q_T is the mass of TNT containing the energy equivalent of the explosive charge in each blasthole (kg). The original equation was modified by Cunningham for ANFO based explosives [14]:

$$X_m = AK^{-0.8} Q_e^{0.167} \left(\frac{S_{ANFO}}{115}\right)^{-0.633} \tag{3}$$

where K is the powder factor (kg/m^3), S_{ANFO} is the weight strength of the explosive relative to ANFO, and Q_e is the mass explosive being used in each hole (kg). The blastability index, originally proposed by Lilly [36], was adopted to determine rock factor:

$$A = 0.06 \times (RMD + JF + RDI + HF) \tag{4}$$

where A is the rock factor, RMD the rock mass description, JF the joint factor, RDI the rock density index and HF the hardness factor. These factors are calculated from geological data such as; in situ block size, joint spacing, joint orientation, rock specific gravity,

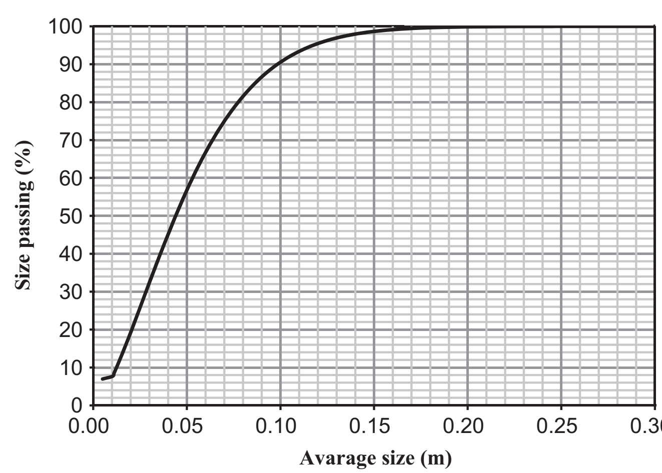

Fig. 4. Muck pile distribution curve for blast No. 9, Sungun copper mine.

Fig. 3. Image analysis for blast no. 9, Sungun copper mine.

Table 2
Basic descriptive statistics of 39 blasts, Sungun copper mine.

No.	Parameter	Symbol	Min	Max	Mean	St.d
1	Burden (m)	B	1.3	5.5	3.94	1.03
2	Maximum instantaneous charge (kg)	MC	81	4230	1404.29	964.78
3	Powder factor (g/ton)	PF	72	373	205.01	171.23
4	S/B ratio	S/B	1	3.9	1.57	1.11
5	S_T/B ratio	S_T/B	0.33	3.44	1.02	0.65
6	Stiffness factor	H/B	1.1	10	3.35	1.91
7	Number of rows	N	1	5	2.64	0.96
8	Time delay (ms)	DLY	20	200	58.10	45.00
9	Hole inclination (degree)	INCL	90	90	90.00	0.00
10	Hole deviation (degree)	DEV	5	15	11.41	2.67
11	Hole diameter	D	125	250	148.39	26.47
12	*J*/*B* ratio	J/B	0	0.45	0.09	0.14
13	Blastability Index	BI	30	63.5	37.61	6.73
14	*B*/*D* ratio	B/D	5	38	26.86	6.70
15	80% passing size	X_{80}	10	108	50.54	21.98

S: Spacing, S_T: Stemming, St. d.: Standard deviation, H: Bench height, Min.: Minimum, Max.: Maximum, Blasting agent is ANFO (0.84 g/cm^3)

Young's modulus and unconfined compressive strength. Cunningham combined the Kuznetsov equation and the Rossin–Rammler distribution to produce the Kuz–Ram model [14]. Since the Kuznetsov formula gives the screen size X_m for 50% of the passing materials, the characteristic size is calculated from the average size by substituting $X=X_m$ and $R=0.5$ into Eq. (1):

$$X_c = \frac{X_m}{(0.693)^{1/n}} \tag{5}$$

The uniformity coefficient is calculated from an equation developed by Cunningham [13]. Cunningham established the applicable uniformity coefficient through several investigations, considering the effect of blast geometry, hole diameter, burden, spacing, hole lengths and drilling accuracy. The *n* factor can be estimated using Eq. (6) given below:

$$n = [2.2 - 14(B/D)]\left[\frac{1+(S/B)}{2}\right]^{0.5}\left(1-\frac{W}{B}\right)\left(\frac{L}{H}\right) \tag{6}$$

where *B* is the blasting burden (m), *S is* the blasthole spacing (m), *D is* the blasthole diameter (mm), *W is* the standard deviation of drilling accuracy (m), *L is* the total charge length (m), and *H* is the bench height (m). Cunningham notes that the uniformity coefficient *n* usually varies between 0.8 and 1.5.

4. Statistical modeling

In reviewing the literatures published, addressing the parameters affecting on the muck pile fragment size [37–41], it is clear that many parameters can influence on the muck pile fragment size. However, the most important parameters, which are easily obtainable, are shown in Table 2. Since, initiation sequence and blast holes pattern are descriptive effective parameters on muck pile fragment size, they were not considered in the statistical modeling.

At the first stage of analysis, hole inclination (INCL) was removed from analysis as it is constant for all blasts with standard deviation of zero (Table 2). The significance of other parameters in the modeling was investigated based upon correlations between the individual independent variables and the actual measured $X_{80.}$ Coefficient of determination (R^2) was used as an indicator of correlation strength. R^2 values for independent variables versus X_{80} are presented in Table 3. It can be concluded that *MC*, *DLY*, *DEV*, *D*, *J*/*B* and *BI* have negligible effects on X_{80} and should be excluded in the regression modeling. Therefore, for further statistical analysis and development of a prediction model, six independent variables were selected.

Table 3
Relations between individual independent variables and X_{80} for 30 blasts, Sungun copper mine.

Independent variables	Regression line	R^2	*N*
B	$X_{80}=16.56(B)-10.27$	0.35	30
MC	$X_{80}=0.002(MC)+48.60$	0.005	30
PF	$X_{80}=-0.142(PF)+74.62$	0.21	30
S/*B*	$X_{80}=-11.61(S/B)+68.48$	0.12	30
S_T/B	$X_{80}=-8.57(ST/B)+60.48$	0.10	30
H/*B*	$X_{80}=-3.60(H/B)+64.17$	0.15	30
N	$X_{80}=10.23(N)+25.54$	0.27	30
DLY	$X_{80}=-0.028(DLY)+52.58$	0.002	30
DEV	$X_{80}=3.44(DEV)+8.29$	0.08	30
D	$X_{80}=0.076(D)+40.39$	0.01	30
J/*B*	$X_{80}=-18.02(J/B)+51.91$	0.01	30
BI	$X_{80}=0.154(BI)+45.44$	0.001	30
B/*D*	$X_{80}=0.916(B/D)+27.07$	0.16	30
Dependant variable: X_{80}			30

4.1. Multiple linear regression analysis

A multiple linear regression analysis was carried out between B, *PF*, *S*/*B*, S_T/B, *H*/*B* and *N* as independent variables and X_{80} as dependent variable, using the commercial software packages for standard statistical analysis (SPSS). Based on the statistical analysis, the predictive model is as follows:

$$X_{80}(\text{cm}) = -32.668+22.160(B)-0.125(PF)+21.264(S/B) +7.979(S_T/B)-3.828(H/B)+9.747(N)-1.801(B/D) \tag{7}$$

A multicollinearity analysis was carried out to check whether two or more independent variables are highly correlated. In the case of occurring multicollinearity, redundancy of the independent variables could be expected, which can lead to erroneous results. One of the most common tools for finding the degree of multicollinearity is the variance inflation factor (VIF). It has a range of 1 to infinity. Generally, if the calculated VIF is greater than 10, there may be a problem with multicollinearity [42]. The VIF values of the independent variables in Eq. (7) were calculated, as shown in Table 4. It was concluded that Eq. (7) with VIF of S_T/B (21.64) and *H*/*B* (27.56) suffers from a high degree of multicollinearity. Also, the relationship between S_T/B and *H*/*B* was

Table 4
Multiple linear regression coefficients and collinearity statistics for Eq. (7).

Independent variables	Unstandardized coefficients		Standardized coefficients	95% Confidence Interval for B		*t* values	Collinearity Statistics	
	B	Std. Error	Beta	Lower Bound	Upper Bound		Tolerance	VIF
Constant	−32.668	49.272		−134.851	69.516	−0.663		
B	22.160	7.258	0.787	7.108	37.212	3.053	0.277	3.604
PF	−0.125	0.068	−0.398	−0.267	0.016	−1.834	0.392	2.552
S/B	21.264	11.412	0.637	−2.402	44.930	1.863	0.158	6.326
S_T/B	7.979	17.682	0.289	−28.691	44.650	0.451	0.045	22.289
H/B	−3.828	6.913	−0.417	−18.165	10.509	−0.554	0.033	30.754
N	9.747	3.773	0.490	1.922	17.572	2.583	0.513	1.949
B/D	−1.081	0.923	−0.400	−2.995	0.834	−1.171	0.158	6.342

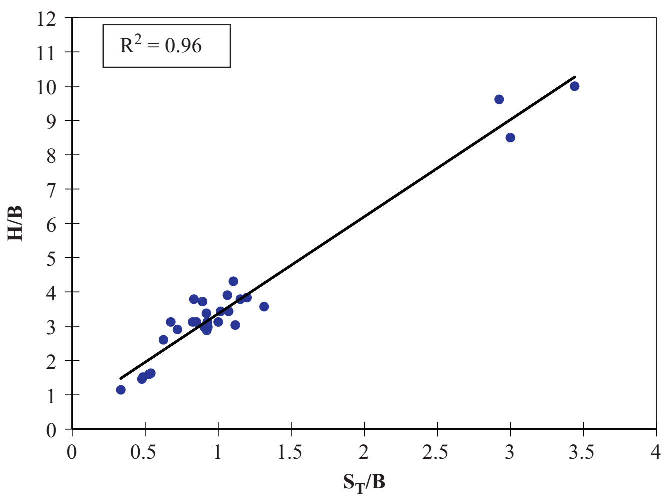

Fig. 5. Correlation between S_T/B and H/B.

Table 5
Regression statistics obtained for Eq. (8).

Model summary					
R	R^2	Adjusted R^2	Std. error of the estimate	Observations	
0.768	0.590	0.483	14.423	30	
Analysis of variance (ANOVA)					
	Sum of squares	df	Mean square	F	Sig.
Regression	6894.923	6	1149.154	5.524	0.001
Residual	4784.543	23	208.024		
Total	11,679.467	29			

examined, which led to finding a high correlation between these two independent variables with determination coefficient (R^2) of 0.96 (Fig. 5).

To reduce the effect of multicollinearity, a new regression model was defined by removing an independent variable from the model that is correlated with another independent variable. Between variables S_T/B and H/B, S_T/B with less determination coefficient (Table 3) was excluded from the model and the new modified model is as follows:

$$X_{80} = -30.278 + 22.229(B) - 0.127(PF) + 20.109(S/B) - 1.130(H/B) + 10.038(N) - 1.180(B/D) \quad (8)$$

The regression statistics, model summary and analysis of variance (ANOVA) for Eq. (8) are shown in Table 5. The model statistic value F and significance (Sig.) are used to provide enough evidence to reject the hypothesis of "no effect". From Table 5, F of 5.52 and Sig. of 0.001 (less than 0.05) were obtained, which show that the null hypothesis can be rejected. It means that at least one of the input parameters significantly affects on the X_{80}. Furthermore, possible multicollinearity of the new model (Eq. (8)) was investigated (Table 6). As it is shown in Table 6, in the modified model, VIF for each independent variable is less than 10. It means that no severe correlation between input independent variables exists.

4.2. Multiple non-linear regression analysis

Polynomial, power, exponential and logarithmic models with the same independent variables and X_{80} as dependent variable and also the same sets of data were used to carry out non-linear regression modeling. The mathematical equation obtained for polynomial model with $R^2 = 0.58$ is

$$X_{80}(\mathrm{cm}) = 11.062 + 10.497(B) - 0.00037(B/D)^2 - 0.00000065(PF)^3 - 0.0505(S/B)^4 + 0.00033(H/B)^5 + 0.0023(N)^6 \quad (9)$$

For power model the relation with $R^2 = 0.58$ is

$$X_{80}(\mathrm{cm}) = 10^{1.332 + 0.152(b) - 0.011(B/D) - 0.001(PF) + 0.121(S/B) - 0.019(H/B) + 0.066(N)} \quad (10)$$

Furthermore, for logarithmic regression modeling, $R^2 = 0.61$ is obtained and the relation is

$$X_{80}(\mathrm{cm}) = 146038 + 53.852\ln(B) - 28.817\ln(B/D) - 14.054(PF) + 26.486(S/B) - 20.350\ln(H/B) + 16.051\ln(N) \quad (11)$$

Finally, the exponential relation for regression modeling with $R^2 = 0.49$ is

$$X_{80}(\mathrm{cm}) = \exp(3.020 + 0.765(B) - 0.105(B/D) - 0.006\,(PF) - 0.098(S/B) + 0.205(H/B) + 0.697(N)) \quad (12)$$

5. Rock engineering systems

The concept of rock engineering systems (RES), introduced by Hudson [43], is a method of structuring all the ways in which rock mechanics parameters and variables can affect one another-the rock mechanics interactions. The key element in the RES is the interaction matrix. The interaction matrix is both the basic analytical and a presentational technique for characterizing the important parameters and the interaction mechanisms in a rock engineering system. The generation of the interaction matrix can help in evaluating the weighting of the parameters within the rock mass system as a whole.

In the interaction matrix, the principal parameters affecting the system (for example, a fragmentation system) are located along the leading diagonal of the matrix and the effects of each individual parameter on any other parameter (interactions) are placed on the off-diagonal cells. The assigning values to off-diagonal cells are called coding the matrix. A problem having only two parameters is the simplest of interaction matrix, as revealed in Fig. 6(a). Also, a general view of the coding of interaction matrix is shown in Fig. 6(b) [43]. The row passing through P_i represents the influence of P_i on all the other parameters in the system, while the column through P_i shows the effects of other parameters, or the remaining of the system, on P_i. In principal, there is no limit to the number of parameters that may be included in an interaction matrix.

Different procedures such as, the 0–1 binary, expert semi-quantitative (ESQ) [43] and the continuous quantitative coding (CQC) [44] were proposed for numerically coding the interaction matrix. Among the coding procedures, the ESQ coding is the most common used. According to this coding technique, the interaction intensity is denoted by the values from 0 (no interaction) to 4 (critical interaction) as shown in Table 7.

In the interaction matrix, the sum of a row is called the "cause" value ($C_{Pi} = \sum_{j=1}^{n} I_{ij}$) and the sum of a column is the "effect" value ($E_{Pj} = \sum_{i=1}^{n} I_{ij}$), denoted as coordinates (C, E) for a particular parameter. The coordinate values for each parameter can be plotted in cause and effect space, forming the so-called C–E plot. The interactive intensity value of each parameter is denoted as the sum of the C and E values ($C+E$) and it can be used as an indicator of parameter's significance in the system. The

Table 7
ESQ interaction matrix coding [43].

Coding	Description
0	No interaction
1	Weak interaction
2	Medium interaction
3	Strong interaction
4	Critical interaction

Table 8
Classification of the vulnerability index (modified after Ref. [33]).

Risk description	Low–medium	Medium–high	High–very high
Category	I	II	III
Vulnerability index	0–33	33–66	66–100

Table 6
Multiple linear regression coefficients and collinearity statistics for Eq. (8).

Independent variables	Unstandardized coefficients		Standardized coefficients	95% Confidence interval for B		t values	Colinearity statistics	
	B	Std. error	Beta	Lower bound	Upper bound		Tolerance	VIF
Constant	−30.278	48.131		−129.845	69.288	−0.629		
B	22.229	7.130	0.790	7.480	36.977	3.118	0.278	3.603
PF	−0.127	0.067	−0.404	−0.265	0.011	−1.897	0.393	2.543
S/B	20.109	10.927	0.602	−2.494	42.713	1.840	0.166	6.007
H/B	−1.130	3.410	−0.123	−8.184	5.924	−0.331	0.129	7.751
N	10.038	3.652	0.505	2.483	17.594	2.748	0.529	1.892
B/D	−1.180	0.881	−0.437	−3.002	0.643	−1.339	0.167	5.984

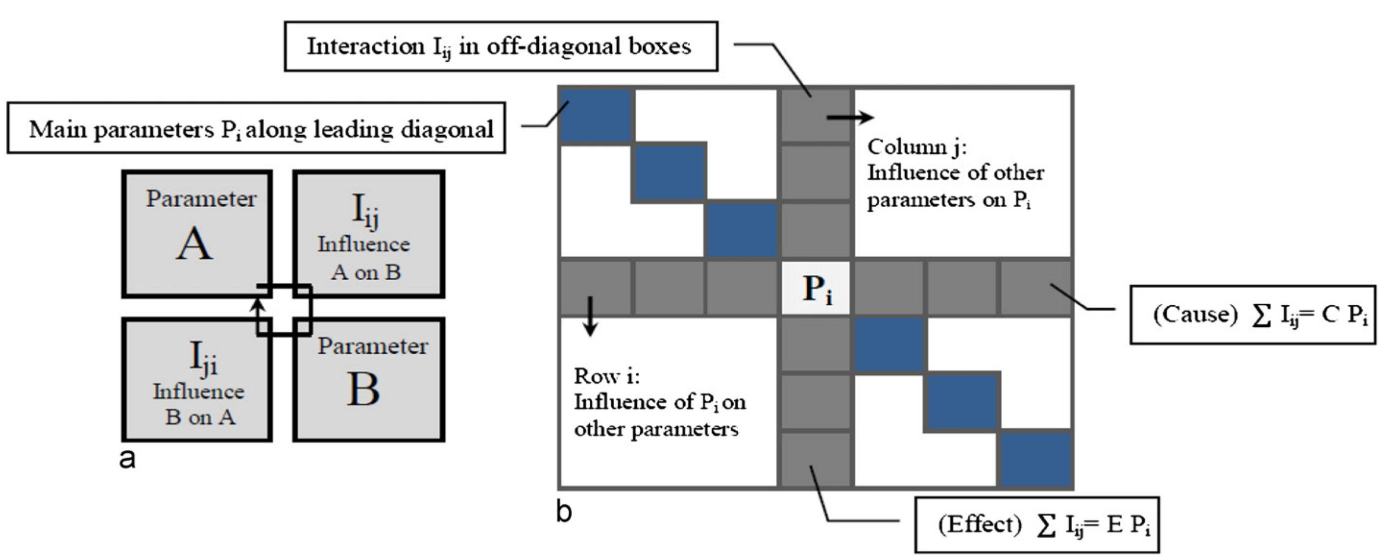

Fig. 6. Interaction matrix in RES, (a) two parameters interaction matrix; (b) a general view of the coding of interaction matrix (modified after Ref. [43]).

percentage value of $(C+E)$ can be used as the parameter's weighting factor (a_i) as follows:

$$a_i = \frac{(c_i + E_i)}{(\sum_i c_i + \sum_i E_i)} \times 100 \qquad (13)$$

6. An RES based model to predict rock fragmentation

The principles of RES were used in the vulnerability index (VI) methodology concept, first introduced by Benardos and Kaliampakos (2004) to identify the vulnerable areas that may pose threat to the tunnel boring machine (TBM) tunneling operation [33]. As there is an obvious relation between advance rate and the associated risk encountered, this concept was also used to predict advance rate in the TBM tunneling. In this research, a similar methodology, inspired by the work carried out by Benardos and Kaliampakos [33] is adopted to define a model, predicting muck pile fragment size, considering poor fragmentation as risk encountered during blasting.

In defining the new model, three main steps must be taken into account. The first step is to identify the parameters that are responsible for the occurrence of risk in case of fragmentation (poor fragmentation), analyze their behavior and evaluate the significance (weight) that each one has in the overall risk conditions (poor fragmentation). In this step, the RES principles can be used to assess the weighting of the parameters involved (within the rock mass system as a whole).

Table 9
Effective parameters used to define the RES based model.

Effective parameters in fragmentation			
P_1	Burden	P_9	Blasthole inclination
P_2	Maximum instantaneous charge	P_{10}	Blasthole deviation
P_3	Powder factor	P_{11}	Hole diameter
P_4	S/B ratio	P_{12}	J/B ratio
P_5	S_T/B ratio	P_{13}	Blast holes pattern
P_6	Stiffness ratio (H/B)	P_{14}	Initiation sequence
P_7	Number of rows	P_{15}	Blastability Index (BI)
P_8	Time delay	P_{16}	B/D ratio

Table 10
The interaction matrix for the parameters affecting on the muck pile fragment size.

P_1	2	2	2	2	2	2	3	2	0	0	2	0	0	0	0
0	P_2	0	0	0	0	0	1	0	0	0	0	0	0	0	0
2	0	P_3	2	0	0	0	0	0	0	0	0	0	0	0	2
0	2	2	P_4	0	0	0	0	0	0	0	0	0	0	0	0
0	2	1	0	P_5	0	0	0	0	0	0	0	0	0	0	0
2	2	2	3	2	P_6	1	1	1	2	2	2	0	0	0	1
1	1	1	0	1	0	P_7	3	0	0	0	0	0	0	0	0
0	1	0	0	0	0	1	P_8	0	0	0	0	0	0	0	0
2	3	2	0	1	0	0	1	P_9	2	0	2	0	0	0	0
2	1	1	2	1	0	0	0	0	P_{10}	0	1	0	0	0	1
3	3	2	1	1	2	1	2	0	3	P_{11}	0	0	1	0	2
0	1	1	0	0	0	0	0	0	0	0	P_{12}	0	0	0	0
2	0	2	2	0	0	1	0	0	0	0	0	P_{13}	2	0	1
2	2	0	1	0	0	2	2	0	0	0	0	0	P_{14}	0	1
3	2	4	2	1	2	2	3	2	3	1	2	2	1	P_{15}	3
3	1	2	0	0	2	1	3	0	0	0	1	1	1	0	P_{16}

In the second step, the vulnerability index can be determined, [33]:

$$VI = 100 - \sum_{i=1} \frac{Q_i}{Q_{\max}} \qquad (14)$$

where a_i is the weighting of the ith parameter, Q_i is the value (rating) of the ith parameter, and Q_{max} is the maximum value assigned for ith parameter (normalization factor)

Based upon the vulnerability index estimated [Eq. (14)] and the classification of the vulnerability index, which is divided into three main categories with different severity of the normalized scale of 0–100 (Table 8) [33], the level of risk corresponding to fragmentation of a blast can be identified. In category I, small-scale problems are expected, that cannot significantly affect the results of fragmentation of the blast. In category II, the problematic occurrence of poor fragmentation might encountered, which must be taken into account. In category III, certain individual regions with poor fragmentation, which might cause several difficulties during the loading, hauling and crushing must be considered.

In the third step, a relation between muck pile fragment size and vulnerability index can be determined. The higher value of VI refers to poor fragmentation and vice versa. Based upon this new

Table 11
Weighting of the principal parameters in rock fragmentation.

No.	Parameters	C	E	$C+E$	$C–E$	a_i (%)
1	Burden	19	22	41	−3	11.7
2	Maximum instantaneous charge	1	22	23	−21	6.6
3	Powder factor	6	22	28	−16	8.0
4	S/B ratio	4	15	19	−11	5.4
5	S_T/B ratio	3	9	12	−6	3.4
6	Stiffness ratio (H/B)	21	8	29	13	8.3
7	Number of rows	7	11	18	−4	5.1
8	Time delay	2	19	21	−17	6.1
9	Blasthole inclination	12	5	17	7	4.9
10	Blasthole deviation	9	10	19	−1	5.4
11	Hole diameter	21	3	24	18	6.9
12	J/B ratio	2	10	12	−8	3.4
13	Blast holes pattern	10	3	13	7	3.7
14	Initiation sequence	10	5	15	5	4.3
15	Blastability index (BI)	33	0	33	33	9.4
16	B/D ratio	15	11	26	4	7.4
	SUM	175	175	350	0	100

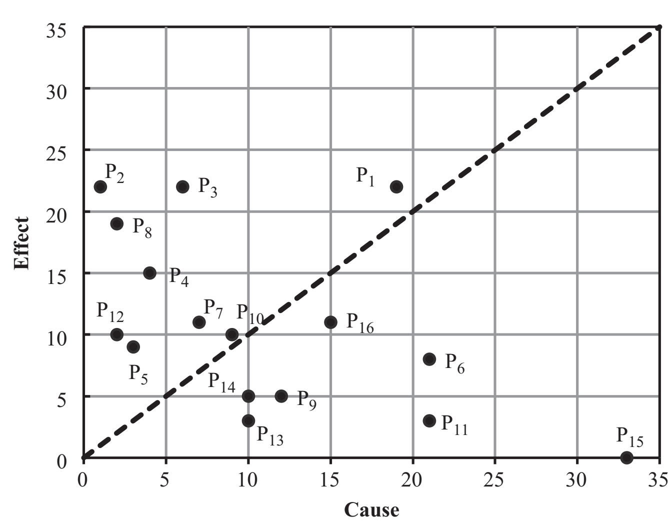

Fig. 7. $E–C$ plot for principal parameters of rock fragmentation.

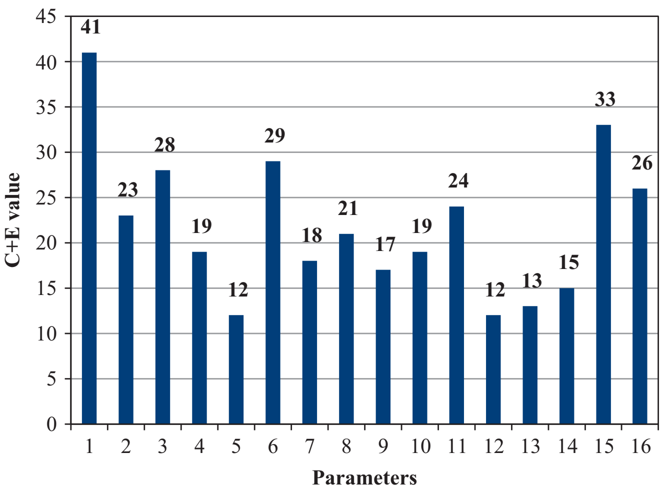

Fig. 8. The $C+E$ values for principal parameters of rock fragmentation.

relation, the muck pile fragment size for every blast can be obtained having VI for the corresponding blast.

6.1. *Effective parameters in the RES based model*

Parameters in Table 2 as well as two descriptive parameters, initiation sequence and blast holes pattern, were used to define the RES based model (Table 9).

6.2. *Interaction matrix and rating of parameters*

6.2.1. *Interaction matrix*

The 16 principal parameters affecting on the muck pile fragment size are located along the leading diagonal of the matrix and the effects of each individual parameter on any other parameter (interactions) are placed on the off-diagonal cells. The assigning values to off-diagonal cells, coding the matrix, were carried out, using the ESQ coding method as proposed by Hudson [43]. Based upon the views of three experts, working in the field of rock blasting for many years,

Table 12
Proposed ranges for the parameters effective in fragmentation.

Parameters		Values/description and ratings						
1	Burden (m)	Value	<3	3–5	5–7	7–9		>9
		Rating	4	3	2	1		0
2	Maximum instantaneous charge (kg)	Value	<500	500–1000	1000–2000	2000–3000	3000–4500	>4500
		Rating	5	4	3	2	1	0
3	J/B ratio	Value	<0.1	0.1–0.3	0.3–0.5	>0.5		
		Rating	0	1	3	2		
4	S/B ratio	Value	<1	1–2	2–3	3–4		>4
		Rating	0	3	2	1		0
5	S_T/B ratio	Value	<0.7	0.7–0.9	0.9–1.2	1.2–1.4		>1.4
		Rating	0	2	4	3		1
6	Number of rows	Value	<3	3–5	5–6	6–7		>7
		Rating	4	3	2	1		0
7	Stiffness ratio (H/B)	Value	>1	1–2	2–3	3–4		>4
		Rating	0	1	2	3		4
8	Blast holes pattern	Description	Staggered	Square	Rectangular	Single row		
		Rating	3	2	1	0		
9	Initiation sequence	Description	V_{34}	V_{64}	$V<_{34}$	V_{45}*		Inter-row
		Rating	4	3	2	1		0
10	Hole deviation (deg.)	Value	0	0–5	5–10	10–15		>15
		Rating	4	3	2	1		0
11	Blastability Index (BI)	Value	0–20	21–40	41–60	61–80		81–100
		Rating	4	3	2	1		0
12	Hole inclination(deg.)	Value	90	90–80	80–70	70–65		>65
		Rating	0	1	2	3		2
13	Powder factor (g/ton)	Value	<125	125–150	150–175	175–210	210–300	<300
		Rating	0	1	2	3	4	4
14	Time delay (ms/m)	Value	<2	2–5	5–7	7–10	10–20	<20
		Rating	0	1	3	4	2	1
15	Hole diameter (mm)	Value	<100	100–150	150–200	200–250	250–300	<300
		Rating	4	3	2	1	0	0
16	B/D ratio	Value	<20		20–40		<40	
		Rating	2		1		0	

* V_{45} denotes the chevron initiation sequence with angle of 45

Table 13
Parameters' values and the corresponding VI for blast shot No. 1, Sungun copper mine.

Parameter	B (m)	MC (kg)	PF (g/ton)	S/B	S_T/B	H/B	N	DLY (ms)	INCL (deg.)	DEV (deg.)	D (mm)	J/B	PAT	SEQ	BI	B/D
Value or description	4	3245	97	1.1	0.9	3	2	50	90	12	125	0	staggered	inter-row	33.5	32
Value rating (Q_i)	3	1	0	3	4	3	4	2	0	1	3	0	3	0	3	1
Weighting (% a_i)	11.7	6.6	8.0	5.4	3.4	8.3	5.1	6.1	4.9	5.4	6.9	3.4	3.7	4.3	9.4	7.4
VI	46															

B: Burden, MC: Maximum instantaneous charge, PF: Powder factor, S: Spacing, S_T: Stemming, H: Height, N: Number of rows, DLY: Time delay, INCL: Hole inclination, DEV: Hole deviation, D: Hole diameter, J: Sub-drilling, PAT: blast holes pattern, SEQ: Initiation sequence, BI: Blasting index.

the interaction matrix for the parameters affecting on the muck pile fragment size is established as presented in Table 10.

Table 11 gives cause (C), effect (E), interactive intensity ($C+E$), dominance (C–E) and weight of each parameter (a_i) for fragmentation purposes. As it can be seen in Table 11, burden has the highest weight in the system, and highly controls other elements. The E–C histogram and $C+E$ for each parameter are illustrated in Figs. 7 and 8, respectively. The points below the $C=E$

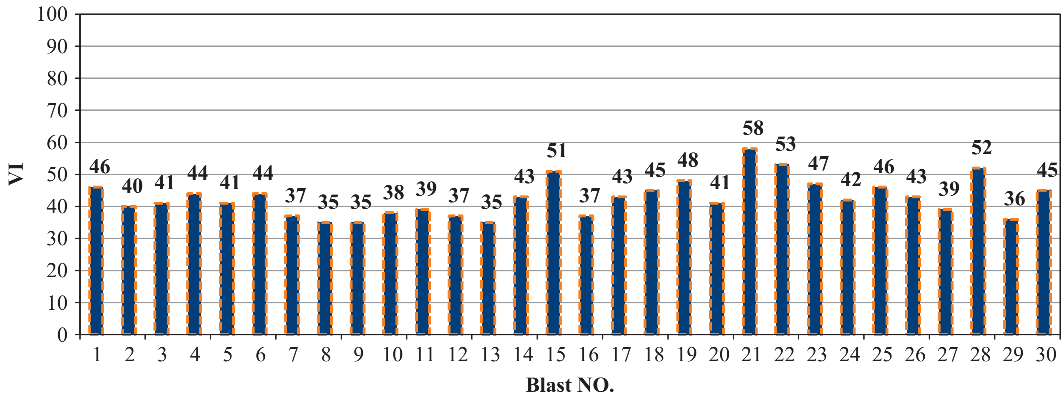

Fig. 9. VI for 30 blasts, Sungun copper mine.

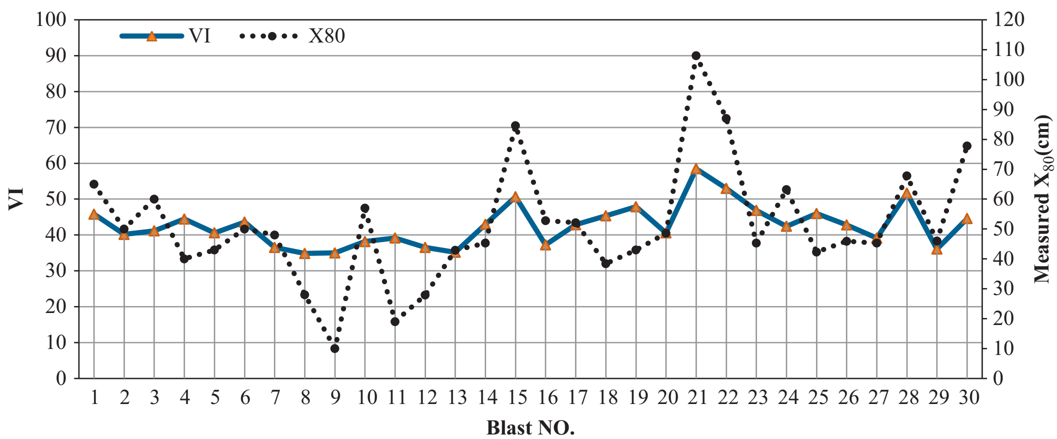

Fig. 10. Agreement between the measured X_{80} and VI for different blasts, Sungun copper mine.

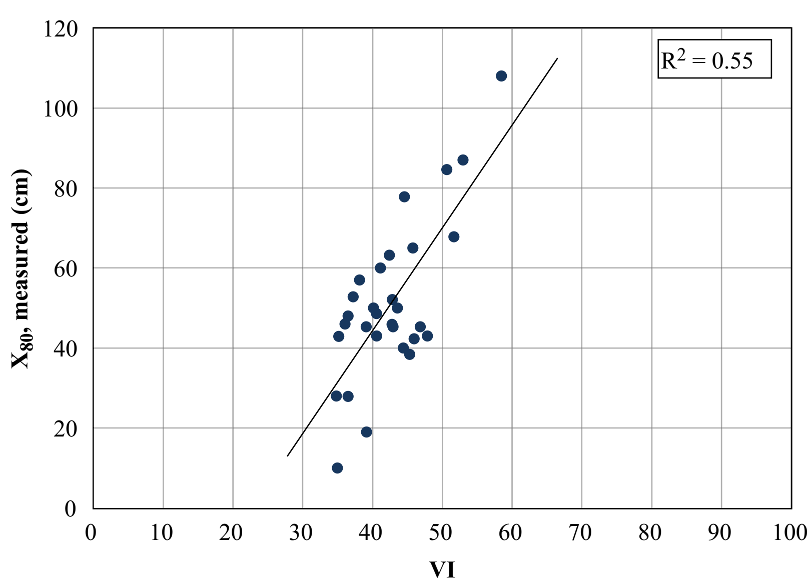

Fig. 11. X_{80}-VI predictive model.

line are called dominant and the points above the $C=E$ line are called subordinate.

6.2.2. Rating of parameters

The rating of the parameter's values was carried out based upon their effect on the muck pile fragment size. Totally six classes of rating, from 0 to 5 were considered, where 0 denotes the worst case (most unfavorable condition (poor fragmentation)) and 5 the best (most favorable condition (good fragmentation)) In the case of rock fragmentation, the rating of each parameter is presented in Table 12. The ranges of parameters in Table 12 were proposed based on the judgments of three experienced experts in the field of rock blasting and also the results obtained by other researchers [37–41].

6.2.3. Risk analysis and fragmentation prediction

The data related to 30 production blasts (out of 39 blasts), carried out at Sungun copper mine, were applied to determine the associated VI for each blast, using Eq. (14). For all blasts, the initiation sequence was inter-row. To make the methodology more understandable, an example of determining VI for blast no. 1 is shown in Table 13. Variations in the VI for the 30 blasts are shown in Fig. 9. As it can be seen, VI varies from 35 to 58, showing that the level of risk is in the second category (Medium–High). Also, there is a good agreement between VI and X_{80} for each blast, as shown in Fig. 10.

Variation in X_{80} with VI for 30 blasts (Fig. 10) suggests a good correlation between X_{80} and VI. Based on the calculated VI and measured X_{80} for 30 blasts, a linear regression analysis was carried out (Fig. 11) and Eq. (15) with coefficient of determination (R^2) of 0.55 was obtained. This relation can be used as a predictive model to predict X_{80} based on VI.

$$X_{80}(\mathrm{cm}) = 2.568(VI) - 58.44 \tag{15}$$

7. Evaluation of models performance

To evaluate the performance of the newly proposed model (RES model), Kuz–Ram and statistical models, nine blasts (out of 39 blasts) carried out at Sungun copper mine were used and the results obtained are shown in Table 14. Also for nine blasts, a comparison was made between the predicted X_{80} and the measured X_{80} for different models as shown in Figs. 12–18.

Two indices, coefficient of determination (R^2) and root mean square error (RMSE) [Eqs. (16) and (17)] were used to carry out the performance analysis of the models and the results obtained are illustrated in Table 15.

$$R^2 = 100\left[\left(\frac{\sum_{i=1}^{n}\left(x_{ipred}-\bar{x}_{ipred}\right)\left(x_{imeas}-\bar{x}_{imeas}\right)\right)^2}{\sqrt{\sum_{i=1}^{n}\left(x_{ipred}-\bar{x}_{ipred}\right)^2\sum_{i=1}^{n}\left(x_{imeas}-\bar{x}_{imeas}\right)^2}}\right)\right] \tag{16}$$

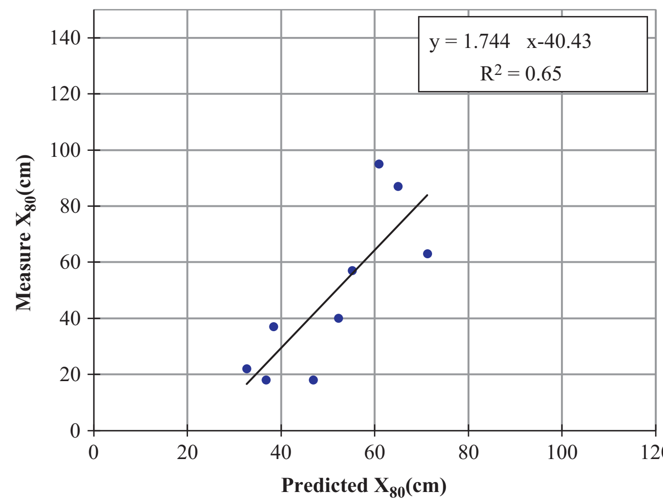

Fig. 12. The measured and predicted X_{80}, RES based model.

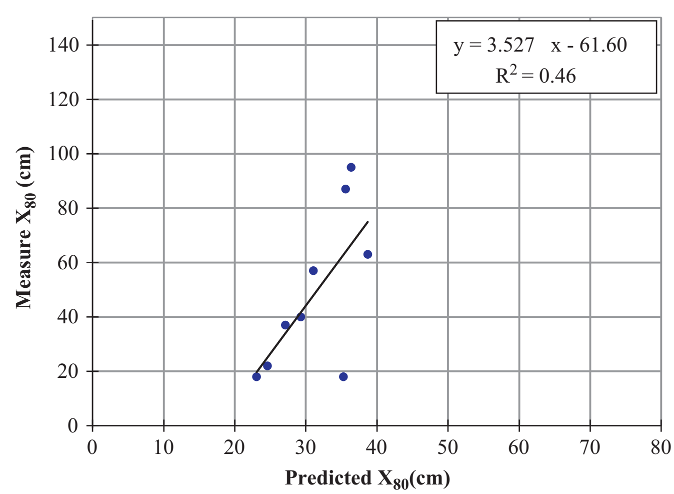

Fig. 13. Comparison between the measured and predicted X_{80}, Kuz–Ram model.

Table 14
X_{80} predicted by various models for nine blasts, Sungun copper mine.

Blast no.	VI	Measured X_{80} (cm)	Predicted X_{80} (cm)						
			RES	Kuz–Ram	Logarithmic	Linear	Power	Polynomial	Exponential
31	46	95	61	36	77	91	100	68	260
32	35	22	33	25	55	56	57	48	117
33	37	18	37	23	55	56	57	48	116
34	38	37	38	27	57	60	61	52	141
35	43	40	52	29	57	61	62	58	84
36	44	57	55	31	68	81	84	67	341
37	51	63	71	39	72	86	92	68	246
38	48	87	65	36	77	95	105	75	441
39	41	18	47	35	71	84	90	68	230

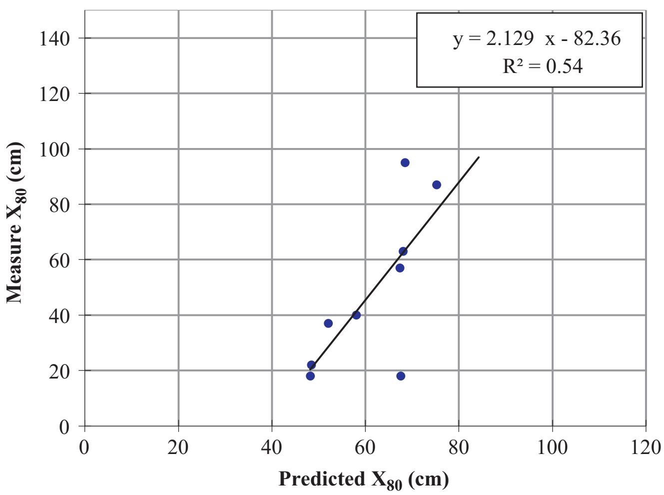

Fig. 14. Comparison between the measured and predicted X_{80}, polynomial model.

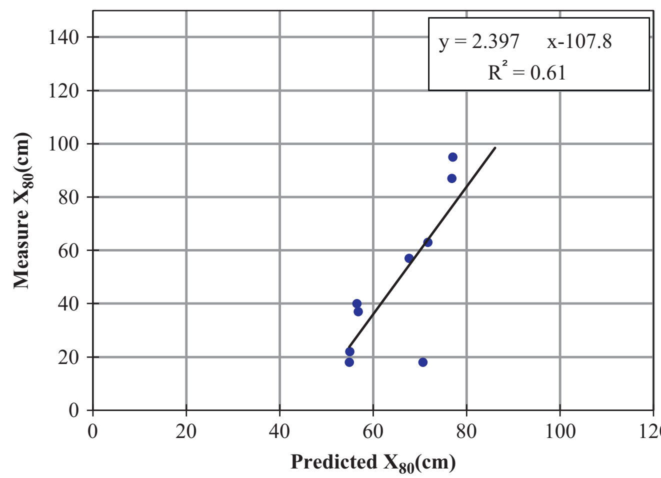

Fig. 17. Comparison between the measured and predicted X_{80}, logarithmic model.

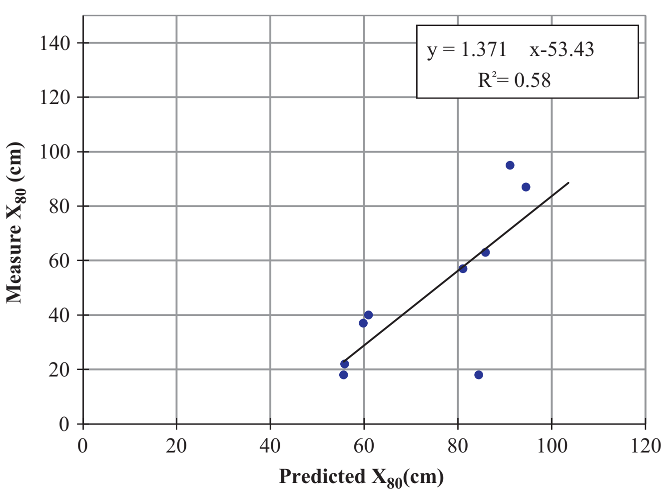

Fig. 15. Comparison between the measured and predicted X_{80}, multiple linear regression model.

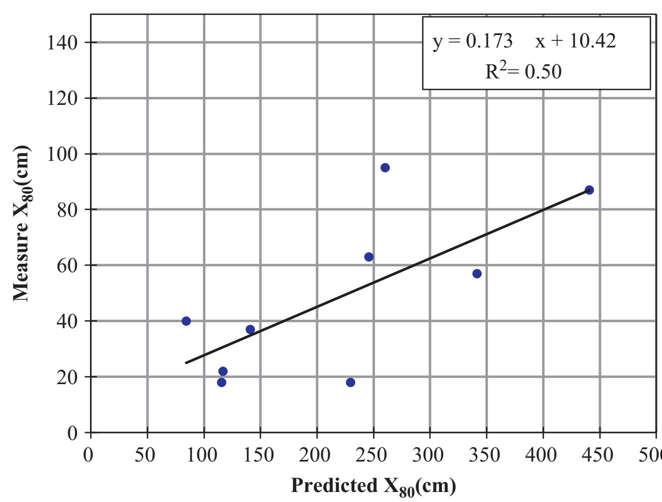

Fig. 18. Comparison between the measured and predicted X_{80}, exponential model.

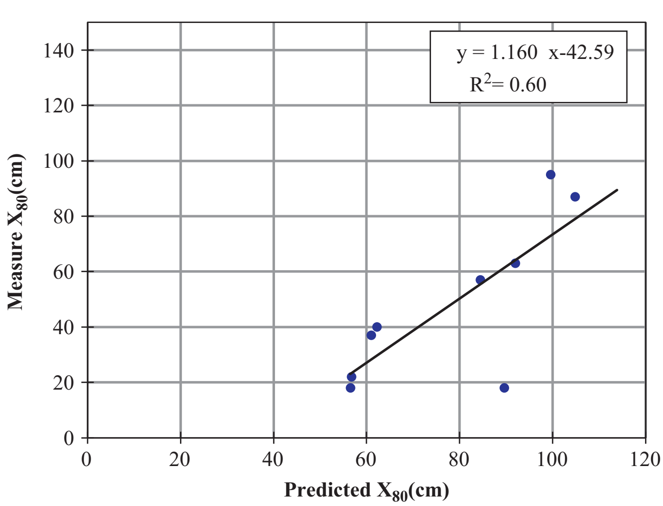

Fig. 16. Comparison between the measured and predicted X_{80}, power model.

$$\mathrm{RMSE}(x) = \sqrt{\frac{1}{n}\sum_{i=1}^{n}\left(x_{imeas} - x_{ipred}\right)^2} \tag{17}$$

Table 15
The results of performance analysis of different models.

Models	R^2	RMSE	Observations
Linear	0.58	29.73	9
Polynomial	0.54	21.58	9
Power	0.60	32.64	9
Logarithmic	0.61	23.80	9
Exponential	0.50	184.60	9
Kuz–Ram	0.46	22.22	9
RES	0.65	14.51	9

where x_{imeas} is the ith measured element, x_{ipred} is the ith predicted element and "n" is the number of datasets.

Furthermore, the predicted X_{80} from Kuz–Ram model, statistical models and RES based model for the nine blasts compared with the measured X_{80} as shown in Fig. 19. As it can be seen from the performance indices (Table 15) and Fig. 19, the RES based model with R^2 of 0.65 and RMSE of 14.51 shows the best agreement with measured X_{80} and works better in comparison with other models. Also it can be seen that the Kuz–Ram model with R^2 of 0.46 but less RMSE shows better performance comparing with some statistical models such as linear, power, logarithmic and exponential. On the other hand, the performance of

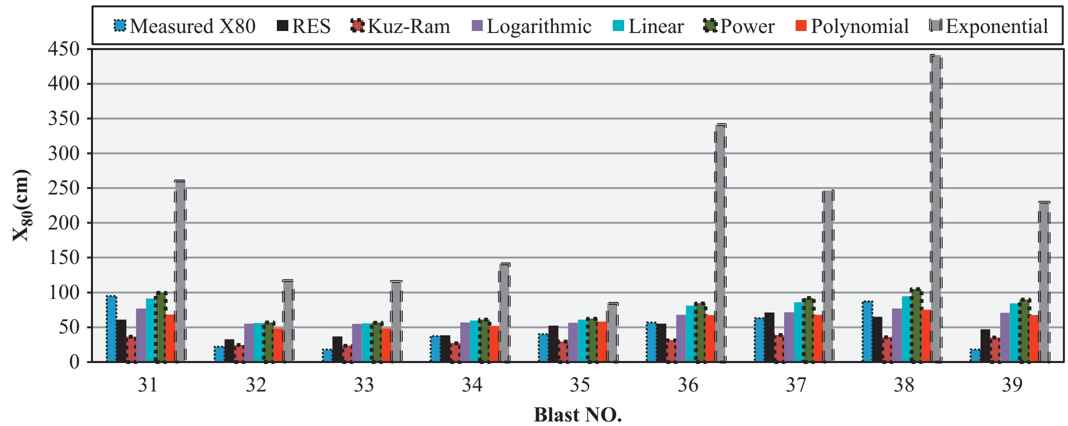

Fig. 19. A comparison between the measured and predicted X_{80} for different models.

exponential model, with R^2 of 0.50 and RMSE of 184.60 has the least consistency with the measured X_{80} and over estimates X_{80}.

8. Conclusions

The RES based model presented in this paper, is an expert based model, which can deal with the inherent uncertainties in the geological systems. Also, it has the privilege of considering unlimited input parameters, which may affect on the system. Moreover, it has the merit of considering descriptive input parameters; for instance, initiation sequence and blast pattern, which are not applicable in statistical modeling.

It is concluded that the RES based model with performance indices, $R^2=0.65$ and RMSE$=14.51$, performs better than linear, polynomial, power, logarithmic, exponential and Kuz–Ram models. It is evident that the prediction model constructed in this research is open for more development if more data are available.

Acknowledgments

The authors wish to thank the Sungun copper mine management for their appreciable cooperation and support, during carrying out this research work.

References

[1] Mackenzie AS. Optimum blasting. In: Proceedings of the 28th annual Minnesota mining symposium. Duluth MN; 1967. p. 181–88.
[2] Mojtabai N, Farmer IW, Savely JP. Optimisation of rock fragmentation in bench blasting. In: Proceedings of the 31th US symposium on rock mechanics. Rotterdam: Balkema; 1990. p. 897–905.
[3] Aler J, Du Mouza J, Arnould M. Measurement of the fragmentation efficiency of rock mass blasting and its mining applications. Int J Rock Mech Min Sci Geomech Abstr 1996;33:125–39.
[4] Aler J, Du Mouza J, Arnould M. Evaluation of blast fragmentation efficiency and its prediction by multivariate analysis procedures. Int J Rock Mech Min Sci Geomech Abstr 1996;33:189–96.
[5] Latham JP, Munjiza A, Lu P. Components in an understanding of rock blasting. In: Proceedings of the 6th international symposium on rock fragmentation by blasting. Johannesburg, South Africa; 1999. p. 173–82.
[6] Jhanwar JC, Jethwa JL, Reddy AH. Influence of air-deck blasting on fragmentation in jointed rocks in an open-pit manganese mine. Eng Geol 2000;57:13–29.
[7] Sanchidrian JA, Segarra P, Lopez ML. Energy components in rock blasting. Int J Rock Mech Min Sci 2007;44:130–47.
[8] Singh DP, Sastry VR. Influence of structural discontinuity on rock fragmentation by blasting. In: Proceedings of the 6th international symposium on intense dynamic loading and its effects. Beijing; 1986.
[9] Ghosh A, Daemen JJK, Van Zyl D. Fractal based approach to determine the effect of discontinuities on blast fragmentation. In: Proceedings of the 31st USA symposium on rock mechanics. Golden, Colo; 1990. p. 905–12.
[10] Kulatilake PHSW W, Hudaverdi T, Kuzu C. Mean particle size prediction in rock blast fragmentation using neural networks. Eng Geol 2010;114:298–311.
[11] Engin I.C. A practical method of bench blasting design for desired fragmentation based on digital image processing technique and Kuz–Ram model. In: Proceedings of the 9th international symposium on rock fragmentation by blasting. Granada, Spain; 2009. p. 257–63.
[12] Kuznetsov VM. The mean diameter of fragments formed by blasting rock. J Min Sci 1973;9:144–8.
[13] Cunningham CVB. The Kuz–Ram model for prediction of fragmentation from blasting. In: Proceedings of the 1st international symposium on rock fragmentation by blasting. Lulea, Sweden; 1983. p. 439–53.
[14] Cunningham CVB. Fragmentation estimations and Kuz–Ram model-four years on. In: Proceedings of the 2nd international symposium on rock fragmentation by blasting. Keystone, Colo; 1987. p. 475–87.
[15] Hjelmberg H. Some ideas on how to improve calculations of the fragment size distribution in bench blasting. In: Proceedings of the 1st international symposium on rock fragmentation by blasting. Lulea, Sweden; 1983. p. 469–94.
[16] Otterness RE, Stagg MS, Rholl SA, Smith NS. Correlation of shot design parameters to fragmentation, In: Proceedings of the international society of explosives engineers. In: Proceedings of the 7th annual conference of explosives and blasting research. Las Vegas; 1991. p. 179–91.
[17] Kou S, Rustan A. Computerized design and result prediction of bench blasting. In: Proceedings of the 4th international symposium on rock fragmentation by blasting. Vienna; 1993. p. 263–71.
[18] Lownds CM. Prediction of fragmentation based on distribution of explosives energy. In: Proceedings of the 11th annual conference of explosives and blasting research. Orlando, Florida, USA; 1995. p. 286–96.
[19] Djordjevic N. Two-component model of blast fragmentation. In: Proceedings of the 6th international symposium on rock fragmentation by blasting. Johannesburg, South Africa; 1999. p. 213–19.
[20] Morin MA, Ficarazzo F. Monte Carlo simulation as a tool to predict blasting fragmentation based on the Kuz–Ram model. Comput Geosci 2006;32:352–9.
[21] Gheibie S, Aghababaei H, Hoseinie SH, Pourrahimian Y. Kuznetsove model's efficiency in estimation of mean fragment size at the Sungun copper mine. In: Proceedings of the 9th international symposium on rock fragmentation by blasting. Granada, Spain; 2009. p. 265–69.
[22] Gheibie S, Aghababaei H, Hoseinie SH, Pourrahimian Y. Modified Kuz–Ram fragmentation model and its use at the Sungun copper mine. Int J Rock Mech Min Sci 2009;46:967–73.
[23] Ouchterlony F. Fragmentation characterization; the Swebrec function and its use in blasting engineering. In: Proceedings of the 9th international symposium on rock fragmentation by blasting. Granada, Spain; 2009. p. 3–22.
[24] Saavedra JC, Katsabanis PD, Pelley CW, Kelebek S. A neural network model for fragmentation by blasting. In: Proceedings of the 8th international symposium on rock fragmentation by blasting. Santiago, Chile; 2006. p. 200–6.
[25] Monjezi M, Rezaee M, Yazdian Varjani A. Prediction of rock fragmentation due to blasting in Gol-E-Gohar iron mine, using fuzzy logic. Int J Rock Mech Min Sci 2009;46:1273–80.
[26] Monjezi M, Bahrami A, Yazdian Varjani A. Simultaneous prediction of fragmentation and flyrock in blasting operation using artificial neural networks. Int J Rock Mech Min Sci 2010;47:476–80.
[27] Chakraborty AK, Raina AK, Ramulu M, Choudhury PB, Haldar A, Sahu P, et al. Parametric study to develop guidelines for blast fragmentation improvement in jointed and massive formations. Eng Geol 2004;73:105–16.
[28] Hudaverdi T, PHSW Kulatilake, Kuzu C. Prediction of blast fragmentation using multivariate analysis Procedures. Int J Numer Anal Meth Geomech 2011;35:1318–33.
[29] Lu P, Hudson JA. A fuzzy evaluation approach to the stability of underground excavations. Proceedings of the ISRM symposium: EUROCK'93 1993:615–22.
[30] Cancelli A, Crosta G. Hazard and risk assessment in rockfall prone areas. In: Skipp B, editor. Risk and reliability in ground engineering. London: Thomas Telford; 1993. p. 177–90.

[31] Mazzoccola DF, Hudson JA. A comprehensive method of rock mass characterization for indicating natural slope instability. Q J Eng Geol 1996;29: 37–56.

[32] Latham JP, Lu P. Development of an assessment system for the blastability of rock masses. Int J Rock Mech Min Sci 1999;36:41–55.

[33] Benardos AG, Kaliampakos DC. A methodology for assessing geotechnical hazards for TBM tunneling-illustrated by the Athens Metro, Greece. Int J Rock Mech Min Sci 2004;41:987–99.

[34] Shin HS, Kwon YC, Jung YS, Bae GJ, Kim YG. Methodology for quantitative hazard assessment for tunnel collapses based on case histories in Korea. Int J Rock Mech Min Sci 2009;46:1072–87.

[35] SRK Consulting Engineers and Scientists. Sungun copper project, mining geotechnics and slope design studies. Final report. Sungun copper company; 2008.

[36] Lilly PA. An empirical method of assessing rock mass blastability. In: Proceedings of the large open-pit conference, IMM. Australia; 1986. p. 89–92.

[37] Langefors U, Kihlstrom B. The modern technique of rock blasting. New York: Wiley; 1978.

[38] Konya CJ, Walter EJ. Rock blasting and overbreak control. FHWA Report-FHWA-HI-92-101; 1991.

[39] Jimeno CL, Jimeno EL, Carcedo FJA. Drilling and blasting of rocks. Rotterdam: Balkema; 1995.

[40] Bhandari S. Engineering rock blasting operations. Rotterdam: Balkema; 1997.

[41] Hustrulid W. Blasting principles for open-pit mining. Rotterdam: Balkema; 1999.

[42] Montgomery DC, Peck EA. Introduction to linear regression analysis. New York: Wiley; 1992.

[43] Hudson JA. Rock engineering systems: theory and practice. Chichester: Ellis Horwood; 1992.

[44] Lu P, Latham JP. A continuous quantitative coding approach to the interaction matrix in rock engineering systems based on grey systems approaches. In: Proceedings of the 7th international congress of IAEG. 1994; p. 4761–70.